Ornamental Plant Research

ARTICLE

Open Access

https://doi.org/10.48130/opr-0025-0009

Ornamental Plant Research **2025**, 5: e007

A comprehensive analysis of the complete *Dendrobium chrysotoxum* mitogenome reveals a multiple-circular structure and horizontal gene transfer from fungi

Cui-Li Zhang[1], Xiong-De Tu[1,2], Lin-Ying Wang[1], De-Qiang Chen[1,2], Meng-Yao Zeng[1], Wei-Lun Yin[1,3], Zhong-Jian Liu[1,2], Xue Liu[4*], Wen-Jun Lin[1,2*] and Si-Ren Lan[1,2*]

[1] *Key Laboratory of National Forestry and Grassland Administration for Orchid Conservation and Utilization at the College of Landscape Architecture and Art, Fujian Agriculture and Forestry University, Fuzhou 350002, China*

[2] *College of Forestry, Fujian Agriculture and Forestry University, Fuzhou 350002, China*

[3] *College of Biological Sciences and Technology, Beijing Forestry University, Beijing 100083, China*

[4] *Chongqing Key Laboratory for the Utilization and Evaluation of Special Chinese Materia Medica Resources, Chongqing Academy of Chinese Materia Medica, Chongqing 400065, China*

* Corresponding authors, E-mail: liu0906xue@163.com; linwenjun@fafu.edu.cn; lkzx@fafu.edu.cn

Abstract

Dendrobium chrysotoxum, a perennial medicinal and horticulture plant in the genus *Dendrobium* within the orchid family (Orchidaceae), holds significant medicinal, ornamental, and scientific value, and thus it is recognized as an innovative horticultural crop. Despite its importance, the mitochondrial genome (mitogenome) of *D. chrysotoxum*, remains unexamined in the current scientific literature. In this study, we assembled an annotation of the complete mitogenome of *D. chrysotoxum*, which comprises 18 circular chromosomes with a total length of 582,418 bp. The mitogenome encodes a total of 63 genes including 37 protein-coding genes (PCGs), three rRNA genes, and 18 tRNA genes. Comparative analyses with other angiosperms revealed variations in gene content. Notably, our analysis revealed the retention of *sdh4* in the *D. chrysotoxum* mitogenome, and it has contracted to 153 bp. Using RNA editing sites, we predicted a total of 605 editing sites across all PCGs, with the *nad4* gene exhibiting the highest number of sites at 57. Our research further identified the extensive presence of mitochondrial plastid DNA sequences, with 87 fragments accounting for 12.75% of the mitogenome. Phylogenetic and synteny analyses further elucidated the evolutionary dynamics and rearrangement events in *D. chrysotoxum* as compared to other *Dendrobium* species. Additionally, we identified a 5,601 bp secondary horizontal gene transfer event involving fungal genes and tRNA genes. Our results provide valuable insights into the symbiotic relationships between orchids and fungi and aids in further research on its potential applications as a medicinal herb with ornamental value.

Citation: Zhang CL, Tu XD, Wang LY, Chen DQ, Zeng MY, et al. 2025. A comprehensive analysis of the complete *Dendrobium chrysotoxum* mitogenome reveals a multiple-circular structure and horizontal gene transfer from fungi. *Ornamental Plant Research* 5: e007 https://doi.org/10.48130/opr-0025-0009

Introduction

Orchidaceae, one of the largest families of angiosperms, represents approximately 10% of all seed plants[1]. Orchidaceae possesses significant medicinal, and ornamental value, and has a key role in advancing botanical and ecological research. Orchids often establish symbiotic relationships with mycorrhizal fungi, which play an essential role in supporting their growth, nutrient uptake, and adaptation to environmental changes[2,3]. Recently, increasing attention has been directed toward the mitochondrial genome (mitogenome) of orchids, a critical component of their genetic makeup. Through genome assembly and annotation, researchers have identified the distinctive structural features and remarkable diversity of orchid mitogenomes[4,5]. Compared to the chloroplast and nuclear genomes, research on the mitogenome of orchids began relatively late. Nevertheless, the mitogenome is crucial for understanding plant biological functions, evolutionary history, and fungal symbiosis mechanisms[6–8].

Recent studies on the mitogenomes of *Dendrobium* species and related orchids have revealed significant differences in gene content, genome size, and structural organization[9,10]. These mitogenomes are often more complex than those of other plant families, characterized by frequent gene rearrangements and occurrences of horizontal gene transfer (HGT) and endosymbiotic gene transfer (EGT)[1,3]. Such phenomena are common within Orchidaceae, suggesting that the mitochondrial genomes of orchids have undergone extensive gene flow and structural changes throughout their evolution. A deeper understanding of these genomic features is essential for developing effective conservation strategies and expanding the use of orchids as ornamental and medicinal crops. Furthermore, orchid mitogenomes often contain complex repeat sequences and subgenomic structures, as highlighted in recent studies[5,11]. While these features complicate genome assembly, they also provide unique insights into plant genome evolution and functionality.

Mitochondria are essential energy supplier units and 'signaling hubs' in eukaryotic cells, providing 90% of the energy required for cellular activities in the form of ATP. They also play a crucial role as signal integrators during plant cell growth, development, and stress response[12,13]. Mitochondria, functioning as semi-autonomously replicating organelles with independent genomes, possess considerable research significance[14]. Mitogenomes are integral to processes such as protein synthesis, transcription, and replication, playing a crucial role in the study of the origin and evolution of organisms[15]. In the evolution of plant mitogenomes, it has been observed that structural evolution occurs more rapidly than sequence evolution. The rate of synonymous substitutions varies across plant genomes. The nuclear genome evolves the fastest, followed by the plastid genome, which evolves at approximately half the rate of the nuclear genome. In contrast, plant mitochondrial genomes evolve several

times more slowly than plastid genomes[16,17]. Analyzing sequence variation in the mitogenome enables the differentiation of species and enhances understanding of their speciation mechanisms, as well as the structure and sequence variation of the genomes during evolution.

Plant mitogenomes are characterized by their large genome size and structural variation, which includes sub-genomic circular structures, polycyclic structures, and complex configurations that can be challenging to resolve. These variations are predominantly composed of non-coding DNA sequences. Due to the unique repair mechanisms in the mitogenome, exogenous DNA sequences can be easily incorporated, leading to the formation of numerous repeated sequences that facilitate homologous recombination[18]. This recombination between homologous sequences generates smaller linear, circular, and multi-branched subgenomes, which coexist alongside the intact primary genome within the cell. The complex structural features of plant mitogenomes have posed significant challenges for their assembly, slowing down sequencing efforts compared to chloroplast DNA (cpDNA).

Despite progress, significant challenges remain in orchid mitochondrial genome research. High structural variability and pronounced differences between species have made the complete assembly of mitogenomes a formidable task. So far, only a few high-quality assemblies have been completed for species within the *Dendrobium*, focusing primarily on preliminary analyses and annotations of key species. However, the available data remain limited, leaving many *Dendrobium* species unstudied. This gap underscores the vast potential for further genomic exploration and phylogenetic analysis. In this study, *Dendrobium chrysotoxum* served as a model for the first assembly and annotation of its mitogenome. *D. chrysotoxum* is a perennial medicinal plant belonging to the genus of *Dendrobium*[19]. Recent research has thoroughly investigated the ornamental and medicinal properties of *D. chrysotoxum*, revealing its considerable potential for development. It is increasingly considered as a promising floral crop with significant value in ornamental, economic, and medicinal sectors within modern agriculture. We conducted a detailed analysis of its structural features, codon bias, RNA editing, HGT, and intracellular gene transfer, comparing the PCGs with those of 21 other angiosperms. Furthermore, we performed collinearity and phylogenetic analyses. The results of this study will establish a solid theoretical foundation for future research, offering new insights into the symbiotic relationships between orchids and fungi. This is crucial for maintaining orchid diversity, horticultural cultivation, and medicinal production.

Materials and methods

Plant materials, DNA extraction, and sequencing

Sample plants of *D. chrysotoxum* were cultivated at the National Orchid Germplasm Resources Center of Fujian Agriculture and Forestry University. Healthy plants were selected, and young leaves were carefully harvested using sterilized tweezers and scissors. The harvested leaves were placed in 5 mL cryovials, immediately frozen in liquid nitrogen, and stored at −80 °C in an ultra-low temperature freezer. DNA was extracted using the CTAB method. The DNA purity, degradation level, and contamination were assessed using a NanoPhotometer® (IMPLEN, CA, USA) and 1% agarose gel. We measured the concentration with a spectrophotometer, Qubit® 3.0 Fluorometer (Life Technologies, CA, USA). After passing quality checks, we prepared a 350 bp DNA fragmentation library. The insert size was verified using an Agilent 2100 platform. Subsequently, the prepared library was sequenced on the NovaSeq 6000 platform using a paired-end sequencing protocol (PE150), which resulted in reads of 150 bp. For long-read sequencing, we used an SQK-LSK110 sequencing kit (Oxford Nanopore Technologies, Oxford, UK) and the PromethION sequencer (Oxford Nanopore Technologies, Oxford, UK) for library construction and sequencing.

Assembly and annotation of *D. chrysotoxum* mitogenome

In this study, we combine Next-Generation Sequencing (NGS) and Long-Read Sequencing technologies, producing 12.5 GB of raw data from the Illumina platform and 14.6 GB of raw data from the Oxford Nanopore platform. To ensure data quality, we removed adapter sequences and low-quality reads from the raw data. For the third-generation sequencing data, we applied the default parameters of Guppy (v5.0) software for filtering, while the second-generation sequencing data were processed with Trimmomatic (v0.39) software to trim adapters and eliminate low-quality reads[20]. Only the resulting high-quality Clean reads were used for all subsequent analyses. We utilized the Flye (v2.9.2-b1786) software with default parameters to directly assemble long reads, resulting in a graphical representation of the mitogenome[21]. The assembled contigs were then subjected to makeblastdb, using mitochondrial genes from *Arabidopsis thaliana* as reference sequences. To identify contigs containing mitogenome sequences, we employed the BLASTn program with specific parameters (-evalue 1e-5 -outfmt 6 -max_hsps 10 -word_size 7 -task blastn-short). For visualization and generation of a draft mitogenome, we used the Bandage (v0.8.1) software[22]. Subsequently, both long reads and short reads were aligned to the identified mitochondrial contigs using bwa (v0.7.17) software, retaining only the aligned reads[23]. Finally, we used Unicycler for assembly with default parameters[24], employing a hybrid assembly strategy to construct the mitogenome of *D. chrysotoxum*. The final mitogenome was then visualized using Bandage (v0.8.1) software[22].

The presence of repetitive sequences often leads to errors in genome assembly, particularly when multiple configurations are possible. In such instances, selecting the correct configuration is crucial. To address repetitive regions within the graphical genome, we prioritize the genome configuration that is supported by the majority of long-reads. When encountering repetitive sequences, especially long reads, we employ the bwa (v0.7.17) software to align them against these sequences[23]. We identify the paths most supported by the long reads to effectively resolve these repetitive areas. This method is also applied to contigs containing multiple junctions to deduce the most probable mitogenome structure. In our case, despite the presence of several repetitive sequences, only one pair of repeats exceeds 1,000 bp - a forward repeat of 2,062 bp located on contig3. Consequently, multiple circular mitochondrial genomes of this species can self-circularize directly without being affected by repetitive sequences. Additionally, the length of our long reads is sufficient to easily span these short repetitive sequences, aiding in obtaining the primary mitogenome configuration. The draft assembled from long-read data was then visualized using the Bandage (v0.8.1) software[22], which resulted in 18 circular genomic DNA sequences.

The mitogenome of *D. chrysotoxum* was annotated using Geseq (v2.03) software, with reference to genomes from *Arabidopsis thaliana* (NC_037304) and *Liriodendron tulipifera* (NC_021152.1)[25]. Additionally, we further annotated the mitogenome of *D. chrysotoxum* using the online tool IPMGA (www.1kmpg.cn/ipmga) and integrated these results with those obtained from the Geseq software. IPMGA was particularly adept at identifying splice sites and trans-splicing genes[26]. tRNA were annotated with the tRNAscan-SE (v.2.0.11) software[27], and rRNAs were annotated using the BLASTN

(v2.13.0) software[28]. Manual corrections of annotation errors were made through the Apollo (v1.11.8) software to ensure meticulousness in annotation accuracy and consistency with established standards in mitogenomics research[29].

Analysis of relative synonymous codon usage and repeated sequences codon bias analysis

We extracted the PCGs from the mitogenome using Phylosuite (v1.1.16)[30]. We performed codon bias analysis and calculation of the relative synonymous codon usage (RSCU) values using MEGA (v7.0)[31]. We employed online tools including MISA (v2.1) (https://webblast.ipk-gatersleben.de/misa/), TRF (v4.09) (https://tandem.bu.edu/trf/trf.unix.help.html), and the REPuter web server (https://bibiserv.cebitec.uni-bielefeld.de/reputer/) to identify repetitive sequences in the mitogenome of *D. chrysotoxum*[32–34]. These tools facilitated the detection of three types of repetitive sequences in mitogenome, simple sequence repeat (SSR), tandem repeats, and dispersed repeats. We visualized the results using Excel (2021) and RCircos (v0.69.9)[35].

Identification of mitochondrial plastid DNA sequences and prediction of RNA editing sites

To identify DNA sequences that migrated from the cpDNA to the *D. chrysotoxum* mitogenome, we assembled the cpDNA using GetOrganelle (v1.6.0)[36]. We used CPGAVAS2 (http://47.96.249.172:16019/analyzer/annotate) to annotate the cpDNA[37], and subsequent corrections were made using CPGView (www.1kmpg.cn/cpgview)[38]. We identified and analyzed candidate homologous fragments between the mitogenome and cpDNA of *D. chrysotoxum* using BLASTN (v2.13.0). The results were visualized with RCircos (v0.69.9)[28,35]. Default parameter settings were used for all software.

To predict C to U RNA editing sites in the 37 PCGs of the mitogenome, we used Deepred-mt, a convolutional neural network (CNN)-based tool. The cutoff value was set at 0.9, and we only considered results with probability values exceeding 0.9 this threshold was considered significant[39].

Identification of mitochondrial horizontal gene transfer (HGT) and gene transferred or lose

To validate the horizontal gene transfer (HGT) events involving fungal genes and tRNA genes, we implemented a multi-step validation approach. Initially, following the method outlined by Sinn & Barrett[3], we downloaded the *Ustilago maydis* (DQ157700) mitogenome from the NCBI database as a reference sequence to search for HGT regions. We sourced the small fungal mitochondrial DNA (FMT) region reference sequences for *Vanilla odorata* and *Apostasia shenzhenica* from Sinn & Barrett[3], while the HGT regions for *U. maydis* and *Vanilla planifolia* were identified by Valencia-D et al.[40] (Supplementary Table S1). To further substantiate our findings, we also referenced large FMT regions from *D. loddigesii*, *Cyrtochilum meirax,* and *Podochilus*_sp, also identified by Valencia-D et al.[40], and the large FMT region sequence of *D. officinale* was identified[3] (Supplementary Table S2). Sequence alignment was conducted using MAFFT (v7.505) to obtain the *D. chrysotoxum* HGT region.

To explore whether these lost genes were transferred to the nuclear genome, we employed the identification method described by Wang et al.[9] to search for these genes within the published nuclear genome of *D. chrysotoxum*[19].

Colinear and phylogenetic analysis

To investigate species evolution, we conducted a comprehensive analysis of collinearity and phylogeny of *D. chrysotoxum*. Using the BLASTn program with the following parameters (e-value 1e-5, word_size 9, gapopen 5, gapextend 2, reward 2, and penalty 3), we identified conserved homologous sequences exceeding 500 bp between the mitogenomes of *D. chrysotoxum* and five other *Dendrobium* species. To visualize the relationships among these genomes, we employed MCscanX (https://github.com/wyp1125/MCScanX) to generate a Multiple Synteny Plot[41].

To analyze phylogeny, we obtained the complete mitogenome sequences from NCBI for a total of 26 species across five angiosperms (Asparagales, Liliales, Arecales, Alismatales, and Ranunculales). Two species from the Ranunculales, *Anemone maxima* (NC 053368.1), and *Aconitum kusnezoffi* (NC 053920.1), served as outgroups. We used PhyloSuite (v1.1.16) software to extract the conserved amino acid sequences of common genes from the mitogenomes of 27 species[30], and multiple sequence alignments were performed using MAFFT (v7.505)[42]. The maximum likelihood (ML) phylogenetic tree was constructed with the IQ-TREE (v1.6.12) software using the parameters (alrt = 1,000, -B = 1,000) to construct the maximum likelihood (ML) phylogenetic tree[43], and the results were visualized using ITOL (v6)[44].

Results

Multiple-circular construction of *D. chrysotoxum* mitogenome assembly and annotation

In this study, we employed a combination of long and short reads to construct the high-quality polycyclic mitogenome of *D. chrysotoxum*. By excluding repetitive regions from the nanopore data, we successfully assembled the multiple-circular mitogenome of *D. chrysotoxum,* revealing 18 circular chromosomes totaling 582,418 bp with a GC content of 43.35% (Fig. 1 & Supplementary Table S3). The lengths of these 18 circular chromosomes vary from 21,961 to 57,950 bp, with the GC content ranging from 39.77% (chromosome 7) to 46.23% (chromosome 4).

A total of 63 genes were annotated, comprising 37 unique PCGs, 23 tRNA genes (14 of which are multicopy), and three rRNA genes. The 37 unique PCGs were made of 24 core genes and 13 variable genes. We categorized the core genes into seven functional types, including five ATP synthase genes (*atp1*, *atp4*, *atp6*, *atp8*, and *atp9*), nine NADH dehydrogenase genes (*nad1*, *nad2*, *nad3*, *nad4*, *nad4L*, *nad5*, *nad6*, *nad7*, and *nad9*), four cytochrome C biogenesis genes (*ccmB*, *ccmC*, *ccmFC*, and *ccmFN*), three cytochrome C oxidase genes (*cox1*, *cox2*, and *cox3*), one protein transport subunit gene (*mttB*), one maturases (*matR*), and one cytochrome b (*cob*). The variable genes encompass two ribosomal protein large subunit genes (*rpl5*, and *rpl16*), 10 ribosomal protein small subunit genes (*rps1*, *rps2*, *rps3*, *rps4*, *rps7*, *rps10*, *rps12*, *rps13*, *rps14*, and *rps19*), one succinate dehydrogenase gene (*sdh4*) (Table 1).

We also examined the conservation of PCGs across 22 angiosperms. To this end, we integrated a variety of factors to select *Amborella trichopoda* as the most basal extant flowering plant. Additionally, *Liriodendron tulipifera*, which has 17 variable genes, and monocotyledon species of *Phoenix dactylifera*, *Allium cepa,* and *Asparagus officinalis* were selected. Furthermore, representative species from five subfamilies of Orchidaceae and eight published species of *Dendrobium* (as of July 1, 2024) were included for comparison. This analysis focused on mitochondrial gene content differences between *D. chrysotoxum* and the other 21 species (Fig. 2). The number and types of PCGs varied across species. For example, *L. tulipifera* had the highest number of PCGs (41), while *A. cepa* had the lowest (24). We found that the *rps8* gene was found to be either completely lost or pseudogenized in all 22 examined species. The *sdh3*, *sdh4*, and *rpl10* genes were universally absent in orchid mitogenomies, except for *sdh4*, which was fully identified in *Paphiopedilum micranthum* and *D. chrysotoxum*. Among the nine

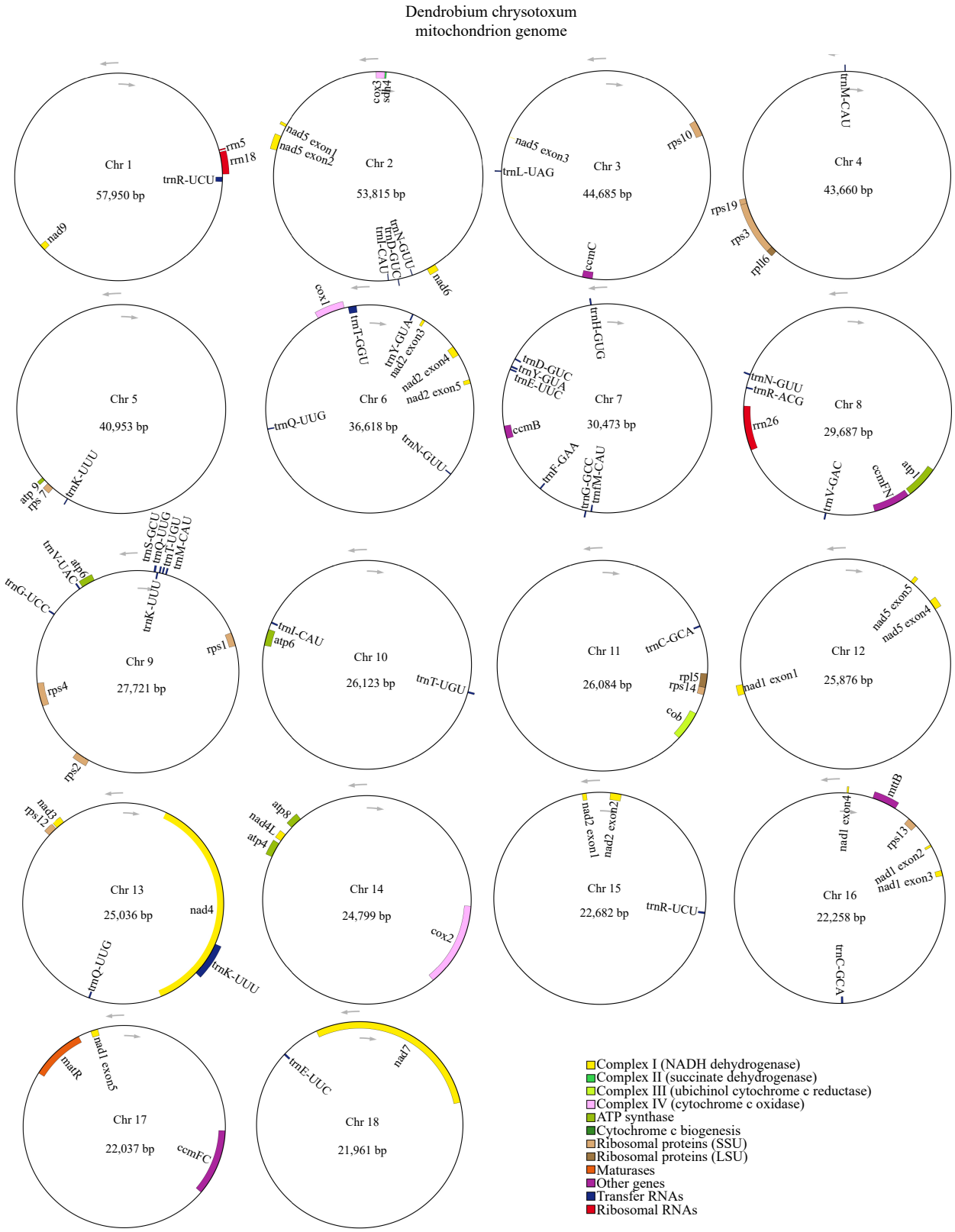

Fig. 1 The mitogenome of *D. chrysotoxum* was represented as a multiple-branching map, consisting of 18 circular chromosomes. Genes transcribed clockwise are depicted inside each circle, while those transcribed counterclockwise are shown outside the circles. Genes are color-coded according to their functional classification.

Dendrobium species analyzed here, we found all 24 core genes were present, with the only exception being a single pseudogene *mttB* in *D. amplum*. Additionally, both *rps11* and *rpl12* genes were absent from the mitogenome of *D. chrysotoxum*.

Additionally, we used the GetOrganelle (v1.6.0) software to assemble the complete cpDNA of *D. chrysotoxum*. The cpDNA displayed a monocyclic structure, totaling 150,607 bp in length. Unlike the mitogenome, the cpDNA features a simpler cyclic structure,

Table 1. Gene contents of the mitogenome of *D. chrysotoxum*.

Group of genes	Name of genes
ATP synthase	*atp1*, *atp4*, *atp6* (×2), *atp8*, *atp9*
NADHdehydrogenase	*nad1*, *nad2*, *nad3*, *nad4*, *nad4L*, *nad5*, *nad6*, *nad7*, *nad9*
Cytochrome b	*cob*
Cytochrome c biogenesis	*ccmB*, *ccmC*, *ccmFC*, *ccmFN*
Cytochrome c oxidase	*cox1*, *cox2*, *cox3*
Maturases	*matR*
Protein transport subunit	*mttB*
Ribosomal protein large subunit	*rpl5*, *rpl16*
Ribosomal protein small subunit	*rps1*, *rps2*, *rps3*, *rps4*, *rps7*, *rps10*, *rps12*, *rps13*, *rps14*, *rps19*
Succinate dehydrogenase	*sdh4*
Ribosome RNA	*rrn5*, *rrn18*, *rrn26*
Transfer RNA	*trnC-GCA*×2, *trnD-GUC*×2, *trn*E-UUC×2, *trnF-GAA*, *trnfM-CAU*, *trnG-GCC*, *trnG-UCC*, *trnH-GUG*, *trnI-CAU*×2, *trnK-UUU*×3, *trnL-UAG*, *trnM-CAU*×2, *trnN-GUU*×3, *trnQ-UUG*×3, *trnR-ACG*, *trnR-UCU*×2, *trnS-GCU*, *trnS-GGA*, *trnT-GGU*, *trnT-UGU*×2, *trnV-GAC*, *trnV-UAC*, *trnY-GUA*×2

consisting of a large single copy (LSC) region, a small copy (SSC) region, and two inverted repeat (IR) sequences (IRA, and IRB). We annotated 110 genes in the cpDNA, including 73 PCGs categorized into 12 functional types, nine rRNA with four rRNA genes (with four duplicated), and 28 tRNA (with 10 tRNA duplicated) (Supplementary Fig. S1 & Supplementary Table S4).

Codon usage of PCGs in *D. chrysotoxum*

Codon usage bias stems from a relative equilibrium within the cell that develops over the long-term evolution of a species. We calculated the relative synonymous codon usage (RSCU) for 37 PCGs in the *D. chrysotoxum* mitogenome. An RSCU value above 1 indicates a preference for a specific amino acid codon. Our analysis revealed that, except the start codon AUG, the tryptophan (Trp) codon UGG, and the serine (Ser) codon AGU (all of which have RSCU values of 1), the mitogenome PCGs of *D. chrysotoxum* generally exhibited a preference for codon usage (Fig. 3 & Supplementary Table S5). Among the mitochondrial PCGs, alanine (Ala) displayed the highest preference with the GCU codon achieving an RSCU value of 1.61. This was followed by the glutamine (Gln) codon CAA and the histidine (His) codon CAU, each with RSCU values of 1.5. A total of 29 A/U-ending codons presented RSCU values above 1, excluding UUG. Additionally, there were 32 codons with RSCU less than 1, with the exceptions of AUA and CUA which ended with C/G bases.

Repeated sequences in the mitochondrial genome of *D. chrysotoxum*

SSRs, a type of tandem repeat sequence with commonly used inheritance characteristics, are frequently utilized in the development of molecular markers. In this study, we identified a total of 148 SSRs from 18 chromosomes. We found that the distribution of these SSRs varied, with chromosome 3 exhibiting the highest number (17) of SSRs (Fig. 4a). The identified SSR repeat fragments were classified based on the number of bases into monomers (A/T), dimers, trimers, tetramers, pentamers, and hexamers. Tetrameric SSRs were the most abundant, comprising 26 types and 51 instances, which accounted for 34.46% of the total SSRs while monomers, dimers, and trimers accounted for 27.03%, 20.95%, and 15.54% of the total SSRs, respectively. Additionally, two pentamers (GATGG/ATCAA) and one hexamer (CATTTC) were identified (Supplementary Table S6).

The three primary types of repetitive sequences in plant cells are SSRs, tandem repeats, and dispersed repeats. In this study, we identified a total of 27 tandem repeat sequences, ranging in length from 24 to 179 bp and in copy number from 1.9 to 5.6. We found that chromosome 5 exhibited the highest number of tandem repeat sequences, totaling 18.52% of all identified tandem repeats. Further, we observed 54 pairs of dispersed repeats (≥ 30 bp) unevenly distributed across 15 chromosomes (Supplementary Table S7). Of these, 41 pairs (75.92%) were direct repeat sequences and 15 pairs (27.78%) were palindromic repeat sequences, with lengths varying from 30 to 2,062 bp. Most dispersed repeats (43 out of 54, 79.63%) had lengths of 30 to 49 bp, with 13 pairs classified as intermediate-sized repeats (50–500 bp) and one pair as a large

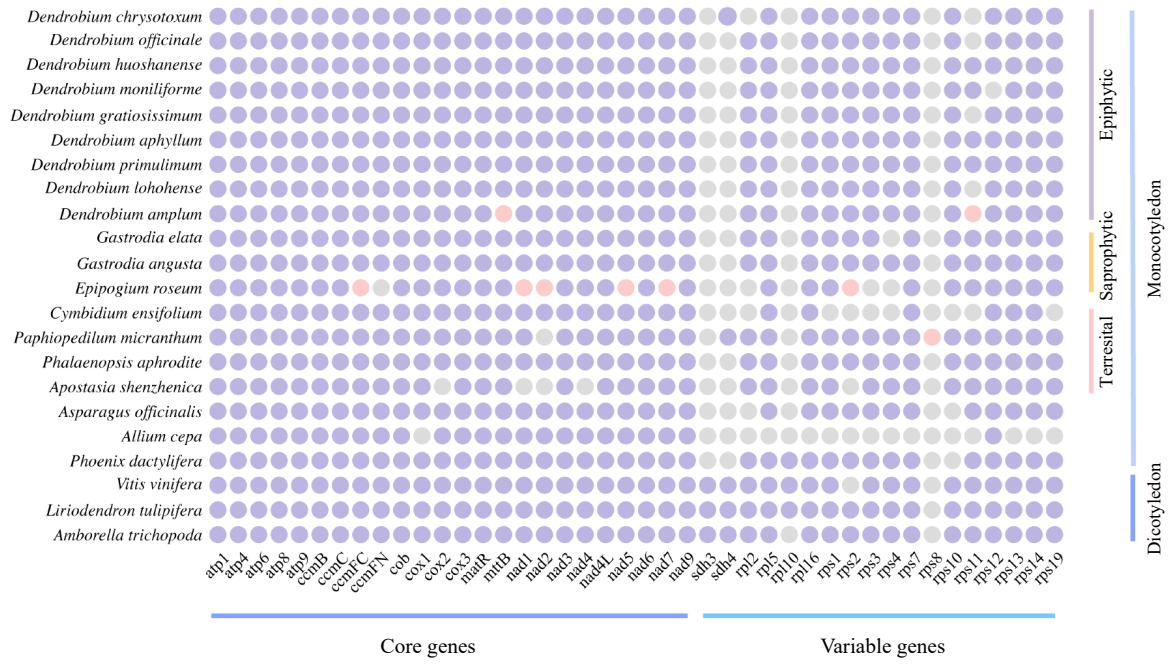

Fig. 2 Comparison of the mitogenome PCGs content of *D. chrysotoxum* and selected angiosperms. Purple indicates present, grey indicates lost, and pink indicates pseudogenes.

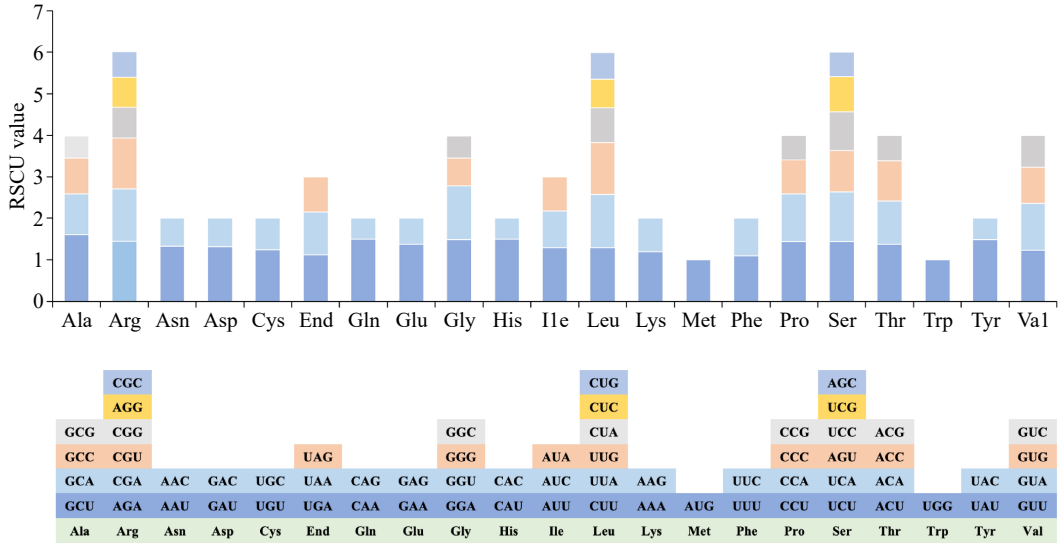

Fig. 3 Analysis of relative synonymous codon usage (RSCU) from *D. chrysotoxum* mitogenome.

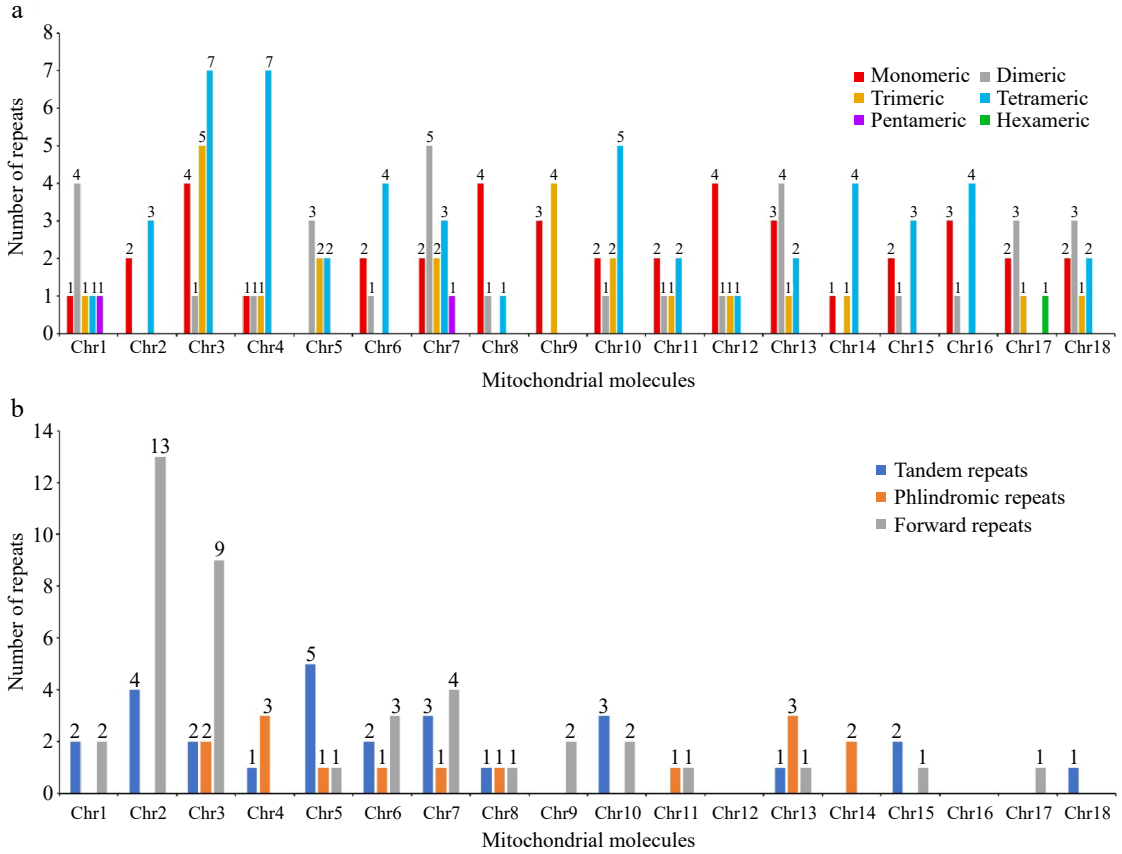

Fig. 4 The repeated sequences in the mitogenome of *D. chrysotoxum*. (a) The SSRs identified in the *D. chrysotoxum* mitogenome. The x-axis indicates mitochondrial molecules. The y-axis indicates the number of repeat fragments. The red legend indicates monomeric SSRs, the gray legend indicates dimeric SSRs, the orange yellow legend indicates trimeric SSRs, the blue legend indicates tetrameric SSRs, the purple legend indicates pentameric SSRs, and the green legend indicates hexametric SSRs. (b) The tandem and dispersed repeats identified in the *D. chrysotoxum* mitogenome. The blue legend said tandem repeats, the yellow legend says palindromic repeats, and the gray forward repeats.

repeat (2,062 bp) (Fig. 4b & Supplementary Table S8). Additionally, some SSRs, interspersed repeats, and tandem repeats were found to overlap (Supplementary Fig. S2).

RNA editing events of *D. chrysotoxum* in 37 PCGs

A total of 605 potential RNA editing sites, converting C to U, were identified across 37 PCGs. The editing sites were unevenly distributed across the genes. The nad4 gene had the highest number of editing sites (57), whereas the rps7, rps10, and sdh4 genes each contained only two. Seven genes (*ccmB*, *ccmC*, *ccmFN*, *nad1*, *nad2*, *nad5*, and *nad7*) each contained 30 or more editing sites (Fig. 5). To assess whether RNA editing exhibited codon position preference, we analyzed the percentage of RNA editing sites as a function of their codon positions. Among all edits observed, first

codon positions were edited 182 times (30.08%), second codon positions were edited 387 times (63.97%), and third codon positions were edited 36 times (5.95%). A total of 44 codons underwent RNA editing events, and the number of edits per codon varied from 1 to 84. The most common transition was from UCA to UUA, which occurred 84 times. Conversely, transitions such as GUC to GUU, AAC to AAU, UAC to UAU, and GGC to GGU occurred only once each in the *D. chrysotoxum* mitogenome. Following RNA editing, the encoded proteins changed as follows, Ser to Leu and Phe, Pro to Ser, Leu, and Phe, Arg to Cys, End, and Trp, His to Tyr, Thr to Ile, and Met, Leu to Phe, Ala to Val. Before the codon shift, the usage frequency of Ser was the highest at 234 (38.6%), while after the codon shift, the usage frequency of Leu was the highest at 268 (44.2%). Additionally, a specific amino acid Arg (CGA) was modified into a stop codon, End (UAA) (Supplementary Table S9).

Identification of mitochondrial plastid sequence and horizontal gene transfer in the mitogenome of *D. chrysotoxum*

During the evolution of mitochondria, sequences from cpDNA have migrated into the mitogenome. In this study, we compare sequences between the mitogenome and cpDNA of *D. chrysotoxum* using BLASTn (v2.13.0) and identified potential mitochondrial plastid DNA sequence (MTPTs) fragments. A total of 87 MTPT fragments were identified, varying in length from 29 bp (MTPT4) to 9,321 bp (MTPT19) with a cumulative length of 74,266 bp, accounting for 12.75% of the total mitogenome length. We found that these homologous sequences were unevenly distributed across 16 chromosomes, excluding Chr11 and Chr16 (Fig. 6a & Supplementary Table S10). Additionally, we validated the HGT event between the *U. maydis* mitogenome and the *D. chrysotoxum* mitogenome (Fig. 6b). We also conducted a comparative analysis of the HGT regions of *D. chrysotoxum* with that of *A. shenzhenica* and *D. officinale*. The identified HGT regions of *D. chrysotoxum* not only included fungal genes consisting of 270 bp from *U. maydis* but also four tRNAs (*trnM-CAU*, *trnS-GCU*, *trnV-UAC*, and *trnG-UCC*) and one ATP synthase gene (*atp6*).

By annotating these MTPT fragments, it was revealed that their origins were both PCGs and tRNA genes within the plastid genome. We identified a total of 31 complete genes, including 20 PCGs (*accD*, *atpB*, *atpE*, *ccsA*, *ndhD*, *ndhE*, *petN*, *psaA*, *psaB*, *psaC*, *psaI*, *psbI*, *psbM*, *psbZ*, *rbcL*, *rpl23*, *rpoB*, *rps14*, *rps16*, and *ycf3*) and 11 tRNA genes (*trnD-GUC*, *trnE-UUC*, *trnfM-CAU*, *trnG-UCC*, *trnH-GUG*, *trnI-CAU*, *trnL-UAG*, *trnM-CAU*, *trnN-GUU*, *trnQ-UUG*, and *trnY-GUA*) (Supplementary Table S10). In addition, our analysis of the diversity of migration sequences revealed 24 intergenic spacers (IGS) within the MTPT fragments, such as *trnF-GAA-ndhJ*, *ndhJ-ndhJ*, *trnT-GGU-psbD*, *trnH-GUG-trnH-GUG*, *rps4-rps4*, *trnN-GUU-trnN-GUU*, *trnN-GUU-rpl32*, *psbJ-psbJ*, *trnR-UCU-trnR-UCU*, *trnG-UCC-trnfM-CAU*, *psbK-psbI*, *rpoB-trnC-GCA*, *ndhJ-trnV-UAC*, *rpl32-trnL-UAG*, *rbcL-accD*, *ndhB-rps7*, *rps7-ndhB*, *ndhJ-trnV-UAC*, *trnS-GGA-trnG-UCC*, *trnS-GGA-trnG-UCC*, *trnT-GGU-psbD*, *trnT-UGU-trnL-UAA*, *matK-rps16*, and *trnN-GUU-trnN-GUU*. In summary, DNA exchange between the mitogenome and cpDNA of *D. chrysotoxum* is significant.

The phylogenomic and colinear of *D. chrysotoxum*

To more accurately describe the evolution of the *D. chrysotoxum* mitogenome, we constructed an ML phylogenetic tree using DNA sequences derived from the 24 core genes. These genes are shared by 26 different angiosperms across five orders, with two mitogenomes from the Ranunculales serving as outgroups (Fig. 7a). The topology of the resulting phylogenetic tree, based on the mitogenome DNA sequence of *D. chrysotoxum*, aligns with the latest Angiosperm Phylogeny Group (APG) classification. Our results demonstrate that *D. chrysotoxum* and *D. officinale* cluster in the same branch, suggesting a more recent common ancestor and indicating a closer relationship between them. In addition, we conducted a collinearity analysis of the mitogenomes of *D. chrysotoxum* and five closely related species using the MCScanX software, focusing on sequence similarity. To enhance the clarity of the results, we excluded collinear blocks smaller than 0.5 kb. Red arcs represent regions of inversion, while gray regions denote highly conserved homologous areas (Fig. 7b). A substantial number of homologous collinear blocks were observed among *D. chrysotoxum* and the five related species. The findings here reveal that the arrangement of collinear blocks across the six mitogenomes is inconsistent, suggesting that *D. chrysotoxum* has undergone genomic rearrangements, resulting in a highly non-conserved order of mitogenome sequences among these species.

Discussion

The mitogenomes of angiosperms are characterized by abundant repetitive sequences and complex circular structures. *Cymbidium ensifolium* mitogenome consists of 19 circular chromosomes and 13.78% (77,244 bp) dispersed repetitive sequences[5]. These repetitive sequences impact the assembly quality of plant mitogenomes, making the assembly of angiosperm mitogenomes particularly challenging[45]. In our study, we utilized a hybrid approach combining Illumina and Oxford Nanopore technologies to assemble the first high-quality complete *D. chrysotoxum* mitogenome of 582,418 bp. Compared to animals (typically a single circular chromosome with < 20 kb) and fungi (17–100 kb)[12,46,47], the size of angiosperm mitogenomes exhibits significant variation, ranging from 66 kb

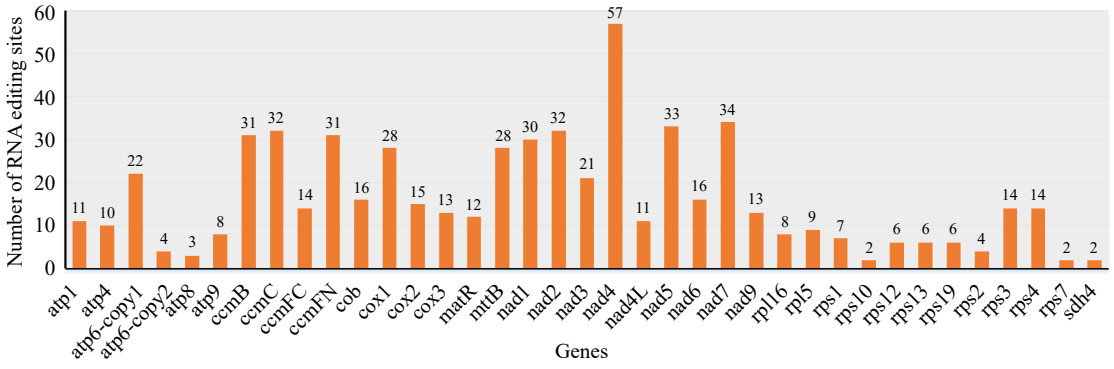

Fig. 5 Prediction of RNA editing sites in mitogenome of *D. chrysotoxum*. The horizontal and vertical coordinates indicate the gene name and the number of RNA edits, respectively.

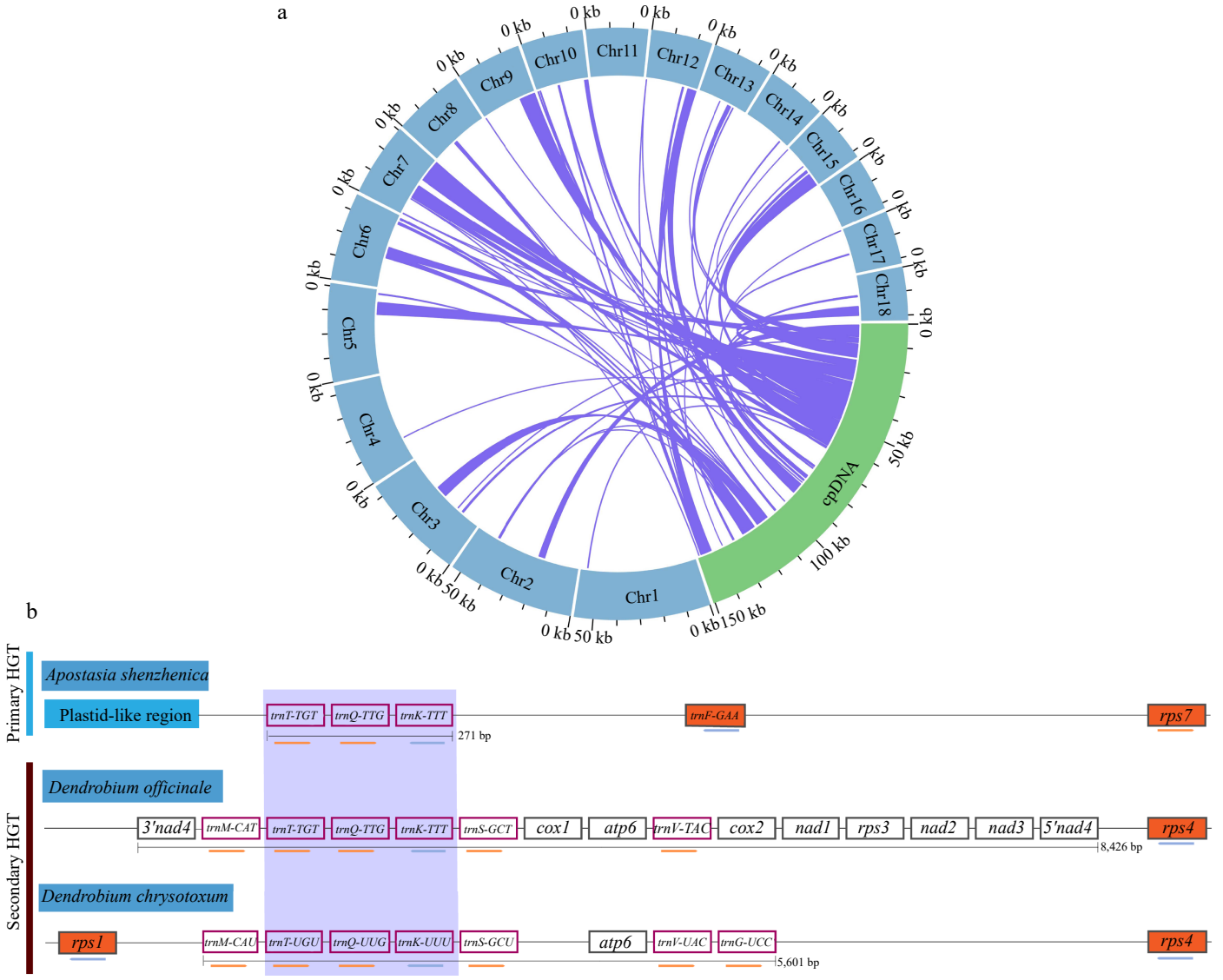

Fig. 6 The intracellular gene transfer and horizontal gene transfer from fungi in the mitogenome of *D. chrysotoxum*. (a) Gene transfer between the cpDNA and mitogenome of *D. chrysotoxum*. Blue represents the mitogenome, the green arc represents cpDNA, and the homologous fragments are indicated using the purple lines between the blue and green arcs. (b) Horizontal gene transfer from fungi in the mitogenome of *D. chrysotoxum*. The purple box highlights the transfer of RNA genes common to all HGTs in three orchids. Orchids plant mitochondrial genes, or nearby plastid-like mitogenomic sequence, is depicted in vermilion, while genes with white backgrounds represent genes of fungal origin, and the coral box represent transfer RNA. The maps are not drawn to scale.

(*Viscum scurruloideum*) to 11.3 Mb (*Silene conica*)[45,48]. The mitogenome of *Dendrobium* showed significant differences from those of other orchids. For example, the mitogenome sizes of various orchids are as follows, *Dendrobium* (420,538–807,551 bp), *Gastrodia elata* (1,340,105 bp), *P. micranthum* (447,368 bp), and *E. roseum* (414,552 bp)[1,9,49,50]. Notably, the mitogenome of *D. chrysotoxum* was different from the other orchid species, despite this, its GC content (43.35%) remains relatively consistent compared to other orchids (43.09%–46.2%), suggesting conserved GC content across orchid mitogenomes.

The number of PCGs in these mitogenomes varies from 19 (*Viscum scurruloideum*) to 41 (*Liriodendron tulipifera*), and the mitogenome of *L. tulipifera,* often referred to as a 'fossil' genome contains 17 variable genes and 24 core genes[25,48]. In this study, the mitogenome of *D. chrysotoxum* lacks at least three PCG genes *sdh3*, *rpl10*, and *rps11*. While *sdh3*, *sdh4*, and *rpl10* were absent from all assembled orchid genomes, the *sdh4* gene is present in the mitogenome of *D. chrysotoxum* and *Paphiopedilum micranthum*. Interestingly, the *sdh4* gene in the *D. chrysotoxum* mitochondria was retained with a length of 153 bp. Similar reductions in the *sdh4* gene sequence have been observed in the mitogenomes of *P. micranthum* (204 bp), *Cocos nucifera* (183 bp), and *Asparagus officinalis* (222 bp)[1].

We investigated whether the missing genes in the *D. chrysotoxum* mitogenome had been transferred to the nuclear or cpDNA by examining published core and assembled cpDNAs[19]. We found the *rps11* genes in the cpDNA and nuclear genome (ID: *Maker45777* and *Maker42721*), but the *rpl10* genes were not in either the nuclear genome or cpDNA. It has been observed that the *rpl10* gene is frequently lost or pseudogenized in angiosperms[51] and in sequenced monocot plants[52], a finding that is consistent with this study. These results indicate that both gene loss and transfer was present in the *D. chrysotoxum* mitogenome. Additionally, the number and sequence conservation of *rps* genes vary significantly between

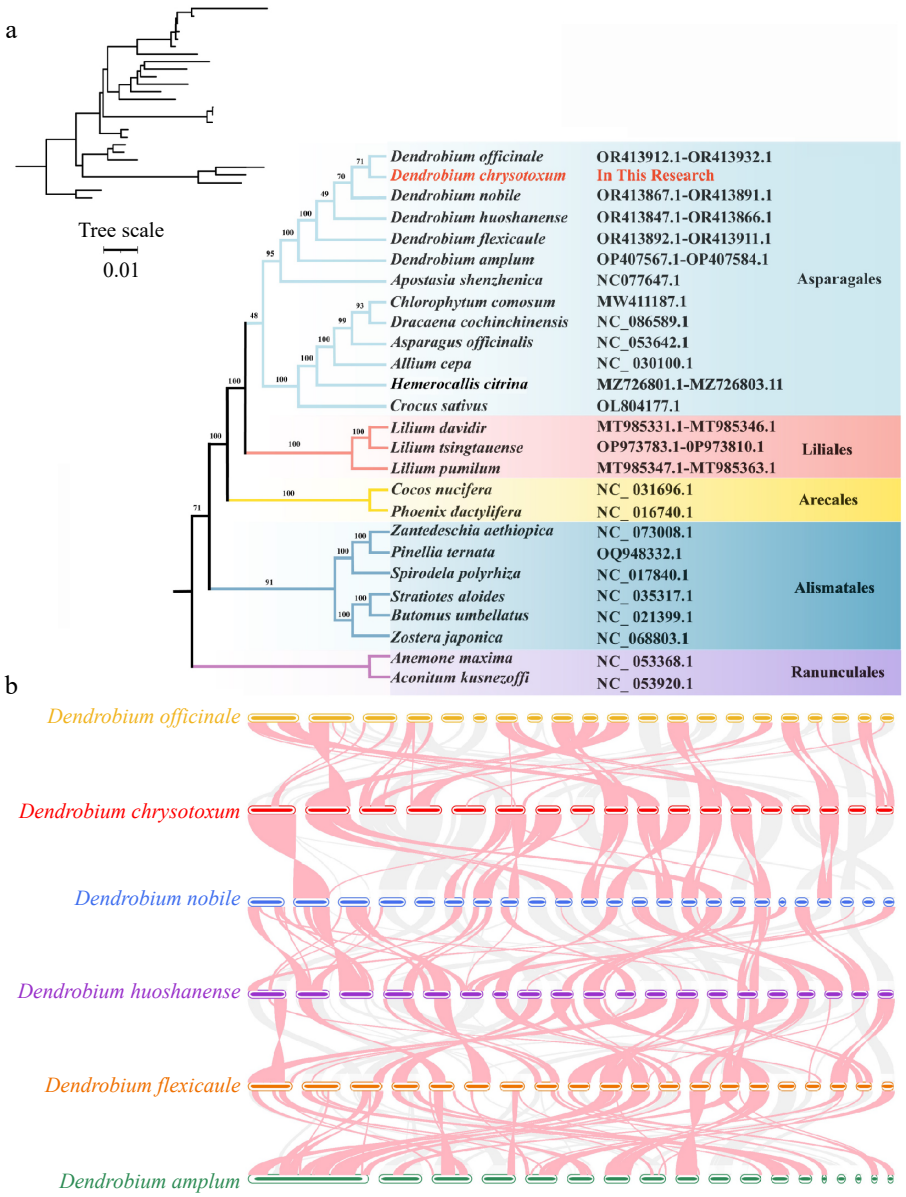

Fig. 7 Phylogenomic and collinear analysis of *D. chrysotoxum*. (a) Construction of the maximum likelihood (ML) tree based on the 26 species. (b) Collinear analysis of the mitogenome of six *Dendrobium* species. The red arcs indicate inverted regions, and the gray arcs indicate better homologous regions.

species[53]. We annotated 10 unique ribosomal protein genes in the mitogenome of *D. chrysotoxum*. The number of *rps* genes contained in the mitogenomes of *Cymbidium ensifolium* and *Allium cepa* was 5 and 1, respectively, which is considerably fewer than in other species. These differences in PCG numbers across these species may be related to the diversity of ribosomal protein small subunit genes.

Repetitive sequences are prevalent in the nuclear, chloroplast, and mitogenomes of angiosperms, influencing their size and structural variation and even mediating mitogenome recombination[54,55]. SSR, tandem repeat, and dispersed repeat are the three main types of repeat sequences in the mitogenome of angiosperms[56,57]. In our study, we identified a multitude of repetitive sequences in *D. chrysotoxum* mitogenome, including a pair of large dispersed repeats (2,062 bp), which potentially contribute to genome expansion. These repetitive sequences may expedite the rearrangement process within the mitogenome. In summary, the abundance of repetitive sequences may accelerate mitogenomic rearrangements in *D. chrysotoxum*.

Angiosperms often include DNA fragments from the plastid genome in their mitogenome[58]. These mitochondrial plastid DNA transfers (MTPTs) play a crucial role in mitogenome assembly[59]. There is a high diversity of MTPTs identified across different species[59,60]. For example, the fragment length and type of MTPTs in the mitogenomes of *D. wilsonii* (79,909 bp, 216–4,227 bp) and *D. henanense* (96,511 bp, 263–9,901 bp) differ significantly[61]. We identified 87 MTPTs in the *D. chrysotoxum* mitogenome, which constitute 12.75% of its total length a proportion that is relatively high compared to other *Dendrobium* species (*D. wilsonii*, 10.5%; *D. henanense*, 12%), and the average level in angiosperms[61]. MTPTs in *D. chrysotoxum* contain complete PCG sequences, which typically lose functionality[62]. We identified 20 PCGs and 11 tRNA genes in these MTPTs fragments, these findings are consistent with annotations in other angiosperms[59].

In addition, the *trnT-TGT*, *trnQ-TTG*, and *trnK-TTT* genes were identified as part of the complete HGT region (270 bp) in both *Apostasia shenzhenica* and *Vanilla planifolia*, referred to as the primary HGT. In

contrast, the 8 kb fungal mitogenome sequence identified in *D. officinale* represents a secondary HGT region[3]. In this study, we identified a 5,601 bp secondary HGT fragment in the Chr9 section of the *D. chrysotoxum* mitogenome, aligning with previous findings[3]. These results suggest that this HGT sequence is conserved. This fragment represents a horizontal transfer from fungal mitogenomes, potentially linked to the symbiotic relationship between orchids and fungi during their early developmental stages. We also examined HGT fragments in other *Dendrobium* species, identifying them in Chr9 of *D. officinale* and in Chr10 of *D. huoshanense*[61]. Therefore, it is hypothesized that *D. chrysotoxum* and *D. officinale* may share a common ancestor. In addition, we retrieved whole-genome sequencing (WGS) data of other *D. chrysotoxum* individuals from the SRA database and subsequently downloaded the PacBio dataset with accession number SRR12823530. This dataset was then aligned to our assembled reference genome, and the results are presented in Supplementary Table S11. Our analysis revealed a substantial number of SNPs and INDELs distributed across both coding and non-coding regions of the genome. Thus, understanding the migration patterns is crucial for elucidating the structural variations of plant mitochondria.

RNA editing is crucial for plant growth and development[39,63]. Additionally, RNA editing facilitates plants' adaptation to various environmental stresses, including drought and high temperatures[64–66]. RNA editing often restores evolutionarily conserved amino acid residues in mRNA or creates translation start and stop codons. This can lead to amino acid substitutions, potentially altering the structure and function of the proteins encoded by the *nad4* gene. For instance, the *ahg11* mutant in *A. thaliana*, which lacks the *nad4* gene, exhibits reduced sensitivity to ABA due to impaired RNA editing. This may affect the nad4 protein's function by altering its electrostatic potential or hydrophobicity. Additionally, in the *mef35-2* Arabidopsis *thaliana* transgenic plants, the RNA editing ability of the *nad4* gene was restored upon introducing the wild-type *MEF35* (*Mitochondrial Editing Factor 35*) gene. In this study, we identified a total of 605 RNA editing sites in the *D. chrysotoxum* mitogenome, with the highest frequency of edits occurring in the second codon position (63.96%), consistent with previous findings in other medicinal plants[59,67]. RNA editing also modifies start and stop codons, underscoring its significance in the regulation of RNA in mitochondrial organelles. During RNA transcriptional regulation, the transcripts of *cox2*, *nad1*, *nad7*, and *rps1* are transferred from ACG to AUG to create the start codon. Similarly, *atp8* and *ccmFC* modify their stop codon through the editing of the CGA codon to UGA. In the mitogenome of *Avena longiglumis*, the *ccmFC* gene undergoes RNA editing to produce stop codons[68]. This process may contribute to maintaining the length stability of protein products encoded by *atp8* and *ccmFC* genes. Thus, predicting RNA editing events provides a potential avenue for unraveling gene functions.

Conclusions

In this study, we have successfully assembled and annotated the first complete mitogenome of *D. chrysotoxum*. We found that the mitogenome is comprised of 18 circular structures totaling 582,418 bp with a GC content of 43.35%. It encodes 63 unique genes, including 37 PCGs. Our analysis highlighted significant aspects such as genome reorganization events, gene content, repetitive sequences, phylogenetic relationships, and RNA-editing sites. The presence of repetitive sequences and identified chloroplast migration sequences in the mitogenome of *D. chrysotoxum* indicate that significant genome reorganization events have occurred during its evolution. The alignment of homologous fragments in the cpDNA, along with the sequence migration fragments identified in this study, suggest extensive DNA exchange. Notably, we identified a 5,601 bp secondary HGT fragment on Chr9, which originated from the *U. maydis* fungal mitogenome. We predicted a total of 605 RNA editing sites in the 37 PCGs, including two sites producing stop codons, which could be a focus for future studies. The construction of the ML phylogenetic tree indicated that *D. chrysotoxum* is closely related to *D. officinale*. These findings enrich the database of *Dendrobium* mitogenomes, providing valuable insights into interspecific relationships, genetic evolution, and the molecular breeding of orchid plants.

Author contributions

The authors confirm contribution to the paper as follows: study conception and design: Zhang CL, Liu X, Lin WJ, Lan SR; data collection: Zhang CL, Tu XD, Wang LY; analysis and interpretation of results: Zhang CL, Chen DQ, Zeng MY; draft manuscript preparation: Zhang CL, Lin WJ; providing suggestions and editing for the manuscript: Yin WL, Liu ZJ. All authors reviewed the results and approved the final version of the manuscript.

Data availability

The assembled mitogenome of *Dendrobium chrysotoxum* has been deposited to GenBank under the accession numbers PP963656–PP963673. The raw data has been released through NCBI with the following accession numbers: BioProject PRJNA1194330, BioSample SAMN45177729, SRA SRR31614518 (Illumina), SRA SRR31614517 (Nanopore). All data generated or analyzed during this study have been included in this published article and its supplementary files and also available from the corresponding author on reasonable request.

Acknowledgments

The research was funded by the National Key Research and Development Program of China (2023YFD1600504), and the Teacher Education Research Project of Fujian Provincial Department of Education (JAT210069).

Conflict of interest

The authors declare that they have no conflict of interest.

Supplementary information accompanies this paper at (https://www.maxapress.com/article/doi/10.48130/opr-0025-0009)

Dates

Received 28 July 2024; Revised 16 December 2024; Accepted 20 December 2024; Published online 25 February 2025

References

1. Yang J, Dierckxsens N, Bai M, Guo Y. 2023. Multichromosomal mitochondrial genome of *Paphiopedilum micranthum*: compact and fragmented genome, and rampant intracellular gene transfer. *International Journal of Molecular Sciences* 24(4):3976
2. Yang Q. 2018. *Study on diversity of Orchidaceae mycorrhizal fungi and its influence on orchid*. Thesis. Chinese Academy of Forestry, China. pp. 81–127
3. Sinn BT, Barrett CF. 2020. Ancient mitochondrial gene transfer between fungi and the orchids. *Molecular Biology and Evolution* 37(1):44–57

4. Wu Z, Liao X, Zhang X, Tembrock LR, Broz A. 2022. Genomic architectural variation of plant mitochondria—a review of multichromosomal structuring. *Journal of Systematics and Evolution* 60(1):160–68
5. Shen B, Shen A, Liu L, Tan Y, Li S, et al. 2024. Assembly and comparative analysis of the complete multichromosomal mitochondrial genome of *Cymbidium ensifolium*, an orchid of high economic and ornamental value. *BMC Plant Biology* 24(1):255
6. Christensen AC. 2013. Plant mitochondrial genome evolution can be explained by DNA repair mechanisms. *Genome Biology and Evolution* 5(6):1079–86
7. Nieuwenhuis M, Groeneveld J, Aanen DK. 2023. Horizontal transfer of tRNA genes to mitochondrial plasmids facilitates gene loss from fungal mitochondrial DNA. *Current Genetics* 69(1):55–65
8. Hou Z, Wang M, Jiang Y, Xue Q, Liu W, et al. 2024. Mitochondrial genome insights into the spatio-temporal distribution and genetic diversity of *Dendrobium hancockii* Rolfe (Orchidaceae). *Frontiers in Plant Science* 15:1469267
9. Wang M, Hou Z, Li C, Yang J, Niu Z, et al. 2023. Rapid structural evolution of *Dendrobium* mitogenomes and mito-nuclear phylogeny discordances in *Dendrobium* (Orchidaceae). *Journal of Systematics and Evolution* 61(5):790–805
10. Wang L, Liu X, Wang Y, Ming X, Qi J, et al. 2024. Comparative analysis of the mitochondrial genomes of four *Dendrobium* species (Orchidaceae) reveals heterogeneity in structure, synteny, intercellular gene transfer, and RNA editing. *Frontiers in Plant Science* 15:1429545
11. Tong W, Yu D, Zhu X, Le Z, Chen H, et al. 2024. The whole mitochondrial genome sequence of *Dendrobium loddigesii* rolfe, an endangered orchid species in China, reveals a complex multi-chromosome structure. *Genes* 15(7):834
12. Liberatore KL, Dukowic-Schulze S, Miller ME, Chen C, Kianian SF. 2016. The role of mitochondria in plant development and stress tolerance. *Free Radical Biology and Medicine* 100:238–56
13. Omelchenko DO, Makarenko MS, Kasianov AS, Schelkunov MI, Logacheva MD, et al. 2020. Assembly and analysis of the complete mitochondrial genome of *Capsella bursa-pastoris*. *Plants* 9(4):469
14. Cheng Y, He X, Priyadarshani SVGN, Wang Y, Ye L, et al. 2021. Assembly and comparative analysis of the complete mitochondrial genome of *Suaeda glauca*. *BMC Genomics* 22:167
15. Dombrovska O, Qiu Y. 2004. Distribution of introns in the mitochondrial gene *nad1* in land plants: phylogenetic and molecular evolutionary implications. *Molecular Phylogenetics and Evolution* 32(1):246–63
16. Wolfe KH, Li WH, Sharp PM. 1987. Rates of nucleotide substitution vary greatly among plant mitochondrial, chloroplast, and nuclear DNAs. *Proceedings of the National Academy of Sciences of the United States of America* 84(24):9054–58
17. Mower JP, Touzet P, Gummow JS, Delph LF, Palmer JD. 2007. Extensive variation in synonymous substitution rates in mitochondrial genes of seed plants. *BMC Evolutionary Biology* 7:135
18. Cole LW, Guo W, Mower JP, Palmer JD. 2018. High and variable rates of repeat-mediated mitochondrial genome rearrangement in a genus of plants. *Molecular Biology and Evolution* 35(11):2773–85
19. Zhang Y, Zhang G, Zhang D, Liu X, Xu X, et al. 2021. Chromosome-scale assembly of the *Dendrobium chrysotoxum* genome enhances the understanding of orchid evolution. *Horticulture Research* 8:183
20. Bolger AM, Lohse M, Usadel B. 2014. Trimmomatic: a flexible trimmer for Illumina sequence data. *Bioinformatics* 30(15):2114–20
21. Kolmogorov M, Yuan J, Lin Y, Pevzner PA. 2019. Assembly of long, error-prone reads using repeat graphs. *Nature Biotechnology* 37(5):540–46
22. Wick RR, Schultz MB, Zobel J, Holt KE. 2015. Bandage: interactive visualization of *de novo* genome assemblies. *Bioinformatics* 31(20):3350–52
23. Li H, Durbin R. 2009. Fast and accurate short read alignment with Burrows-Wheeler transform. *Bioinformatics* 25(14):1754–60
24. Wick RR, Judd LM, Gorrie CL, Holt KE. 2017. Unicycler: resolving bacterial genome assemblies from short and long sequencing reads. *PLoS Computational Biology* 13(6):e1005595
25. Richardson AO, Rice DW, Young GJ, Alverson AJ, Palmer JD. 2013. The "fossilized" mitochondrial genome of *Liriodendron tulipifera*: ancestral gene content and order, ancestral editing sites, and extraordinarily low mutation rate. *BMC Biology* 11:29
26. Shan Y, Li J, Duan X, Zhang X, Yu J. 2024. Elucidating the multichromosomal structure within the *Brasenia schreberi* mitochondrial genome through assembly and analysis. *BMC Genomics* 25(1):422
27. Lowe TM, Eddy SR. 1997. tRNAscan-SE: a program for improved detection of transfer RNA genes in genomic sequence. *Nucleic Acids Research* 25(5):955–64
28. Chen Y, Ye W, Zhang Y, Xu Y. 2015. High speed BLASTN: an accelerated MegaBLAST search tool. *Nucleic Acids Research* 43(16):7762–68
29. Lewis SE, Searle SMJ, Harris N, Gibson M, Iyer V, et al. 2002. Apollo: a sequence annotation editor. *Genome Biology* 3(12):research0082.1
30. Zhang D, Gao F, Jakovlić I, Zou H, Zhang J, et al. 2020. PhyloSuite: an integrated and scalable desktop platform for streamlined molecular sequence data management and evolutionary phylogenetics studies. *Molecular Ecology Resources* 20(1):348–55
31. Kumar S, Stecher G, Tamura K. 2016. MEGA7: molecular evolutionary genetics analysis version 7.0 for bigger datasets. *Molecular Biology Evolution* 33(7):1870–74
32. Benson G. 1999. Tandem repeats finder: a program to analyze DNA sequences. *Nucleic Acids Research* 27(2):573–80
33. Kurtz S, Choudhuri JV, Ohlebusch E, Schleiermacher C, Stoye J, et al. 2001. REPuter: the manifold applications of repeat analysis on a genomic scale. *Nucleic Acids Research* 29(22):4633–42
34. Beier S, Thiel T, Münch T, Scholz U, Mascher M. 2017. MISA-web: a web server for microsatellite prediction. *Bioinformatics* 33(16):2583–85
35. Zhang H, Meltzer P, Davis S. 2013. RCircos: an R package for Circos 2D track plots. *BMC Bioinformatics* 14(1):244
36. Jin JJ, Yu WB, Yang JB, Song Y, DePamphilis CW, et al. 2020. GetOrganelle: a fast and versatile toolkit for accurate de novo assembly of organelle genomes. *Genome Biology* 21:241
37. Shi L, Chen H, Jiang M, Wang L, Wu X, et al. 2019. CPGAVAS2, an integrated plastome sequence annotator and analyzer. *Nucleic Acids Research* 47(W1):W65–W73
38. Liu S, Ni Y, Li J, Zhang X, Yang H, et al. 2023. CPGView: a package for visualizing detailed chloroplast genome structures. *Molecular Ecology Resources* 23(3):694–704
39. Edera AA, Small I, Milone DH, Sanchez-Puerta MV. 2021. Deepred-Mt: deep representation learning for predicting C-to-U RNA editing in plant mitochondria. *Computers in Biology and Medicine* 136:104682
40. Valencia-D J, Neubig KM, Clark DP. 2023. The origin and fate of fungal mitochondrial horizontal gene transferred sequences in orchids (Orchidaceae). *Botanical Journal of the Linnean Society* 203(2):162–79
41. Wang Y, Tang H, DeBarry JD, Tan X, Li J, et al. 2012. *MCScanX*: a toolkit for detection and evolutionary analysis of gene synteny and collinearity. *Nucleic Acids Research* 40(7):e49
42. Katoh K, Standley DM. 2013. MAFFT multiple sequence alignment software version 7: improvements in performance and usability. *Molecular Biology and Evolution* 30(4):772–80
43. Nguyen LT, Schmidt HA, Von Haeseler A, Minh BQ. 2015. IQ-TREE: a fast and effective stochastic algorithm for estimating maximum-likelihood phylogenies. *Molecular Biology and Evolution* 32(1):268–74
44. Letunic I, Bork P. 2019. Interactive Tree Of Life (iTOL) v4: recent updates and new developments. *Nucleic Acids Research* 47(W1):W256–W259
45. Zimmer M, Lückemann G, Lang BF, Wolf K. 1984. The mitochondrial genome of the fission yeast *Schizosaccharomyces pombe*: 3. Gene mapping in strain EF1 (CBS 356) and analysis of hybrids between the strains EF1 and *ade7–50h*. *Molecular and General Genetics MGG* 196:473–81
46. Cummings DJ, McNally KL, Domenico JM, Matsuura ET. 1990. The complete DNA sequence of the mitochondrial genome of *Podospora anserina*. *Current Genetics* 17:375–402
47. Sloan DB, Alverson AJ, Chuckalovcak JP, Wu M, McCauley DE, et al. 2012. Rapid evolution of enormous, multichromosomal genomes in flowering plant mitochondria with exceptionally high mutation rates. *PLoS Biology* 10(1):e1001241
48. Skippington E, Barkman TJ, Rice DW, Palmer JD. 2015. Miniaturized mitogenome of the parasitic plant *Viscum scurruloideum* is extremely divergent and dynamic and has lost all nad genes. *Proceedings of the National Academy of Sciences of the United States of America* 112(27):E3515–E3524

49. Yuan Y, Jin X, Liu J, Zhao X, Zhou J, et al. 2018. The *Gastrodia elata* genome provides insights into plant adaptation to heterotrophy. *Nature Communications* 9(1):1615
50. Zhao Z, Li Y, Zhai J, Liu Z, Li M. 2024. Organelle genomes of *Epipogium roseum* provide insight into the evolution of mycoheterotrophic orchids. *International Journal of Molecular Sciences* 25(3):1578
51. Mower JP. 2020. Variation in protein gene and intron content among land plant mitogenomes. *Mitochondrion* 53:203–13
52. Mower JP, Bonen L. 2009. Ribosomal protein L10 is encoded in the mitochondrial genome of many land plants and green algae. *BMC Evolutionary Biology* 9:265
53. Zhang K, Wang Y, Zhang X, Han Z, Shan X. 2022. Deciphering the mitochondrial genome of *Hemerocallis citrina* (Asphodelaceae) using a combined assembly and comparative genomic strategy. *Frontiers in Plant Science* 13:1051221
54. Schnable PS, Ware D, Fulton RS, Stein JC, Wei F, et al. 2009. The B73 maize genome: complexity, diversity, and dynamics. *Science* 326(5956):1112–15
55. Li J, Li J, Ma Y, Kou L, Wei J, et al. 2022. The complete mitochondrial genome of okra (*Abelmoschus esculentus*): using nanopore long reads to investigate gene transfer from chloroplast genomes and rearrangements of mitochondrial DNA molecules. *BMC Genomics* 23:481
56. Yang Z, Ni Y, Lin Z, Yang L, Chen G, et al. 2022. *De novo* assembly of the complete mitochondrial genome of sweet potato (*Ipomoea batatas* [L.] Lam) revealed the existence of homologous conformations generated by the repeat-mediated recombination. *BMC Plant Biology* 22(1):285
57. Liu D, Guo H, Zhu J, Qu K, Chen Y, et al. 2022. Complex physical structure of complete mitochondrial genome of *Quercus acutissima* (Fagaceae): a significant energy plant. *Genes* 13(8):1321
58. Dong S, Chen L, Liu Y, Wang Y, Zhang S, et al. 2020. The draft mitochondrial genome of *Magnolia biondii* and mitochondrial phylogenomics of angiosperms. *PLoS One* 15(4):e0231020
59. Jiang M, Ni Y, Li J, Liu C. 2023. Characterisation of the complete mitochondrial genome of *Taraxacum mongolicum* revealed five repeat-mediated recombinations. *Plant Cell Reports* 42(4):775–89
60. Wang D, Wu YW, Shih ACC, Wu CS, Wang YN, et al. 2007. Transfer of chloroplast genomic DNA to mitochondrial genome occurred at least 300 MYA. *Molecular Biology and Evolution* 24(9):2040–48
61. Wang M, Yu W, Yang J, Hou Z, Li C, et al. 2023. Mitochondrial genome comparison and phylogenetic analysis of *Dendrobium* (Orchidaceae) based on whole mitogenomes. *BMC Plant Biology* 23(1):586
62. Rice DW, Alverson AJ, Richardson AO, Young GJ, Sanchez-Puerta MV, et al. 2013. Horizontal transfer of entire genomes via mitochondrial fusion in the angiosperm *Amborella*. *Science* 342(6165):1468–73
63. Tang W, Luo C. 2018. Molecular and functional diversity of rna editing in plant mitochondria. *Molecular Biotechnology* 60(12):935–45
64. Rieder LE, Savva YA, Reyna MA, Chang YJ, Dorsky JS, et al. 2015. Dynamic response of RNA editing to temperature in *Drosophila*. *BMC Biology* 13:1
65. Rodrigues NF, da Fonseca GC, Kulcheski FR, Margis R. 2017. Salt stress affects mRNA editing in soybean chloroplasts. *Genetics and Molecular Biology* 40:200–08
66. Riemondy KA, Gillen AE, White EA, Bogren LK, Hesselberth JR, et al. 2018. Dynamic temperature-sensitive A-to-I RNA editing in the brain of a heterothermic mammal during hibernation. *RNA* 24(11):1481–95
67. Zhang D, Zhao X, Li Y, Ke S, Yin W, et al. 2022. Advances and prospects of orchid research and industrialization. *Horticulture Research* 9:uhac220
68. Liu Q, Yuan H, Xu J, Cui D, Xiong G, et al. 2023. The mitochondrial genome of the diploid oat *Avena longiglumis*. *BMC Plant Biology* 23(1):218